Influence of pH on the Equilibrium Association Constants for Oligodeoxyribonucleotide-Directed Triple Helix Formation at Single DNA Sites†

Scott F. Singleton and Peter B. Dervan*

Arnold and Mabel Beckman Laboratories of Chemical Synthesis, Division of Chemistry and Chemical Engineering, California Institute of Technology, Pasadena, California 91125

Received July 10, 1992

ABSTRACT: The energetics of oligodeoxyribonucleotide-directed triple helix formation for the pyrimidine·purine·pyrimidine structural motif were determined over the pH range 5.8–7.6 at 22 °C (100 mM Na^+ and 1 mM spermine) using quantitative affinity cleavage titration. The equilibrium binding constants for 5′-TTTTTCTCTCTCTCT-3′ (**1**) and 5′-TTTTTm^{5}CTm^{5}CTm^{5}CTm^{5}CTm^{5}CT-3′ (**2**, m^{5}C is 2′-deoxy-5-methylcytidine) increased by 10- and 20-fold, respectively, from pH 7.6 to 5.8, indicating that the corresponding triple-helical complexes are stabilized by 1.4 and 1.7 kcal·mol^{-1}, respectively, at the lower pH. Replacement of the five cytosine residues in **1** with 5-methylcytosine residues to yield **2** affords a stabilization of the triple helix by 0.1–0.4 kcal·mol^{-1} over the pH range 5.8–7.6. An analysis of these data in terms of a quantitative model for a general pH-dependent equilibrium transition revealed that pyrimidine oligonucleotides with cytidine and 5-methylcytidine form local triple-helical structures with apparent pK_a's of 5.5 (C+GC triplets) and 5.7 (m^{5}C+GC triplets), respectively, and that the oligonucleotides should bind to single sites on large DNA with apparent affinity constants of $\sim 10^6$ M^{-1} even above neutral pH.

Oligonucleotide-directed triple helix formation provides a versatile structural motif for the design of molecules capable of sequence-specific recognition of double-helical DNA (Moser & Dervan, 1987; LeDoan et al., 1987; Cooney et al., 1988). Pyrimidine oligodeoxyribonucleotides bind in the major groove of double-helical DNA parallel to a purine-rich strand of the Watson-Crick duplex to form a local pyrimidine·purine·pyrimidine triple-helical structure (Moser & Dervan, 1987; Praseuth et al., 1988; de los Santos et al., 1989; Rajagopal & Feigon, 1989a,b). The sequence specificity for the binding of an oligonucleotide to its double-helical target site is achieved through the formation of specific hydrogen bonds between the pyrimidine bases of the third strand and the purine bases of the duplex. Hoogsteen pairing of thymine (T) in the third strand with adenine (A) of a Watson–Crick AT base pair allows formation of T·AT base triplets (Figure 1) (Felsenfeld et al., 1957; de los Santos et al., 1989; Rajagopal & Feigon, 1989a,b). An isomorphous C+GC triplet results from the Hoogsteen-type interactions between an N3-protonated cytosine (C+) in the third strand and a guanine (G) of a Watson–Crick GC base pair (Figure 1) (Howard et al., 1964; de los Santos et al., 1989; Rajagopal & Feigon, 1989a,b; Live et al., 1991). In addition, there are other triple-helical structural motifs, such as the purine·purine·pyrimidine motif (Cooney et al., 1988; Beal & Dervan, 1991), that can be utilized for sequence-specific DNA recognition.

The stabilities of local pyrimidine·purine·pyrimidine triple-helical complexes at single sites on relatively large DNA (>200 bp) are dependent on length, sequence composition, and base sequence mismatches (Moser & Dervan, 1987; Mergny et al., 1991; Roberts & Crothers, 1991; Singleton & Dervan, 1992; Kiessling et al., 1992). Moreover, the solution conditions, including pH, temperature, and the identity and concentration of cations, contribute to the absolute stabilities of these complexes (Moser & Dervan, 1987; Maher et al., 1990). Triple-helical nucleic acids containing cytosines in the third strand are stable in acidic to neutral solutions, but they dissociate as the pH increases (Lee et al., 1979; Moser & Dervan, 1987; Lyamichev et al., 1988; Povsic & Dervan, 1989; Maher et al., 1990; Plum et al., 1990). Apparently, an important factor in the stability of triple-helical complexes is the protonation at cytosine N3 in the third strand, which enables the formation of two hydrogen bonds and provides for partial charge neutralization.

The potential application of oligonucleotide-directed triple helix formation to the specific repression of eukaryotic gene expression in vivo, where the pH is strictly regulated, has stimulated recent efforts to stabilize the protonated C+GC triplets by modification of the oligonucleotide (Povsic & Dervan, 1989) and to design nucleosides capable of GC base pair recognition without protonation (Ono et al., 1991; Koh & Dervan, 1992; Krawczyk et al., 1992). For example, replacing the cytosines in the third strand with 5-methylcytosines (m^{5}C's) increased both the apparent stabilities and upper pH limits of complexes resulting from oligonucleotide-directed triple helix formation (Povsic & Dervan, 1989). This substitution, in which a single –H to –CH_3 change has been affected on the opposite side of the heterocycle from the hydrogen-bonding sites (Figure 1), maintains the same array of potential hydrogen-bond donors and acceptors found in cytosine and results in minimal perturbation of the electronic structure (Sober, 1970). Despite the apparent similarity of C and m^{5}C, the incorporation of m^{5}C has proven to be important in the use of oligonucleotides as inhibitors of site-specific DNA binding by proteins near pH 7 (Maher et al., 1989, 1990; Strobel & Dervan, 1991; Strobel et al., 1991; Collier et al., 1991; Grigoriev et al., 1992; Duval-Valentin et al., 1992).

It has been demonstrated that the substitution of m^{5}C for C increases the thermal stabilities of both polynucleotide (Lee et al., 1984) and oligonucleotide triplexes (Plum et al., 1990). More recently, the heats of denaturation of triple-helical complexes formed by an oligonucleotide hairpin duplex and oligonucleotide third strands containing C or m^{5}C have been

† This research was supported by National Institutes of Health Grant GM-35724 and by a Ralph M. Parsons Foundation predoctoral fellowship to S.F.S.

0006-2960/92/0431-10995$03.00/0

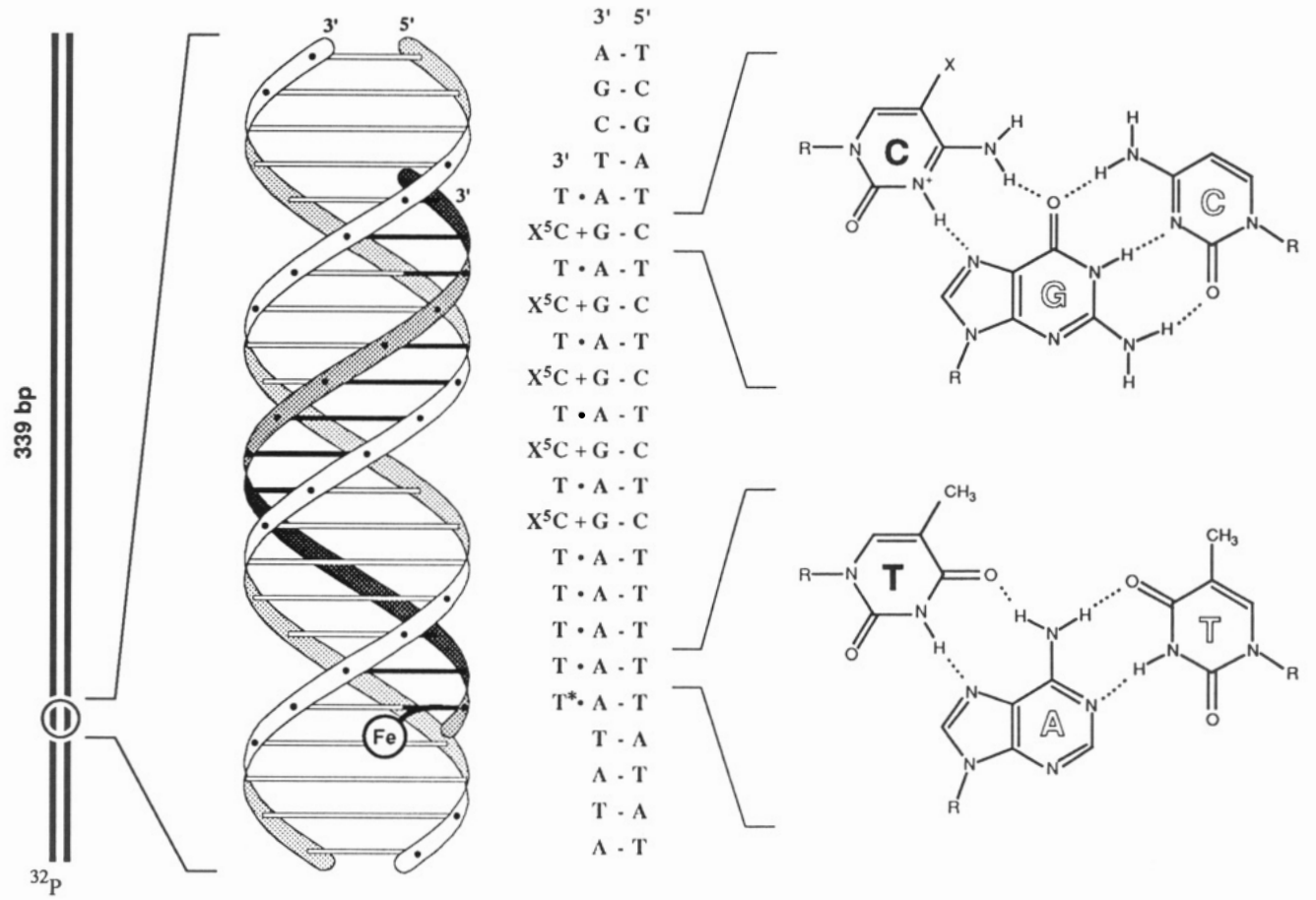

FIGURE 1: (Left) Ribbon model of the local triple-helical structure formed by the binding of **1** to the 15 bp target sequence within the 339 bp end-labeled duplex. The Watson–Crick duplex strands are depicted as white ribbons, while the oligonucleotide–EDTA·Fe is depicted as a dark ribbon. The sequences modeled by the ribbons are shown in the center. (Right) Two-dimensional models depicting the X^{5}C+GC and T·AT base triplets formed by Hoogsteen-type hydrogen bonding of N3-protonated C (X = H) or m^{5}C (X = CH_3) to a Watson–Crick GC base pair (top) and by Hoogsteen hydrogen bonding of T to a Watson–Crick AT base pair (bottom), respectively. The bases of the third strand are labeled with dark type, and the bases of the Watson-Crick duplex are labeled with outline type.

reported (Xodo et al., 1991). We are interested in the measurement of equilibrium association constants for oligonucleotide-directed triple helix formation at individual DNA sites as a first step in understanding the factors contributing to the stability and specificity of triple-helical complexes. We report the influence of pH on the energetics of oligonucleotide-directed triple helix formation using quantitative affinity cleavage titration (Singleton & Dervan, 1992). By measuring the amounts of site-specific cleavage produced by two oligonucleotide–EDTA·Fe conjugates, 5′-TTTTT-CTCTCTCTCT-3′ (**1**, Figure 2) and 5′-TTTTTm^{5}CTm^5-CTm^{5}CTm^{5}CTm^{5}CT-3′ (**2**), over a range of concentrations spanning 4 orders of magnitude, we have constructed empirical titration binding isotherms and determined equilibrium constants for site-specific DNA binding at 22 °C (100 mM Na^+, 1 mM spermine) over the pH range of 5.8–7.6. These affinity cleavage titration experiments have been used to measure the effects of pH and C → m^{5}C substitution on the stability of a local triple-helical complex at a single site on large DNA.

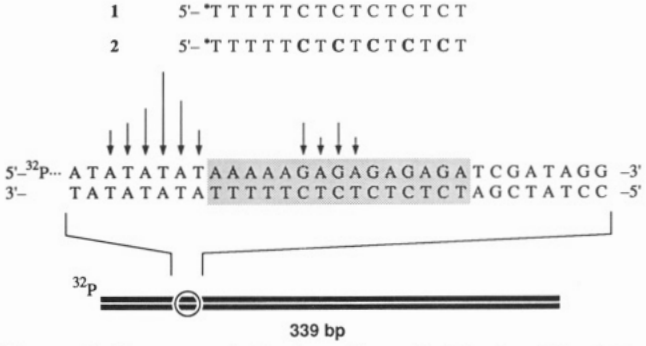

FIGURE 2: Sequences of oligodeoxyribonucleotides **1** and **2**, where T* indicates the position of thymidine–EDTA·Fe and bold type indicates 5-methylcytidine nucleosides. The sequence of the 15 bp target site (shaded box) is shown below, along with the relative position of the target site within the radiolabeled duplex. The arrows indicate the nucleotide positions which are cleaved most efficiently by oligodeoxyribonucleotides **1** and **2**, and the lengths of the arrows are proportional to the relative cleavage efficiency produced by **1** at the designated position at 22 °C and pH 7.0.

MATERIALS AND METHODS

Materials. Sonicated, deproteinized calf thymus DNA (Pharmacia) was dissolved in H_2O to a final concentration of 2.0 mM in base pairs and was stored at 4 °C. Glycogen was obtained from Boehringer-Manheim as a 20 mg/mL aqueous solution. Nucleotide triphosphates were Pharmacia Ultra-Pure grade and were used as supplied. Nucleoside triphosphates labeled with ^{32}P (≥5000 Ci/mmol) were obtained from Amersham. Cerenkov radioactivity was measured with a Beckman LS 2801 scintillation counter. DNase I was purchased from Pharmacia. All other enzymes were purchased from New England Biolabs and were used according to the supplier's recommended protocol in the activity buffer provided. Thymidine and 2′-deoxycytidine phosphoramidites were purchased from ABI. 2′-Deoxy-5-methylcytidine phos-

phoramidite was supplied by Cruachem. The pH of the equilibration solutions was measured as follows: a 1-mL solution containing all buffer and salt components (except radiolabeled DNA) at concentrations identical to those used in the reactions was prepared and equilibrated at the reaction temperature, and the pH of the buffer-salt solution was recorded using a digital pH/millivolt meter (model no. 611, Orion Research) and a ROSS semimicro combination pH electrode (model no. 81-15, Orion Research). General manipulations of duplex DNA (Sambrook et al., 1989) and oligonucleotides (Gait, 1984) were performed according to established procedures.

DNA Preparation. Oligodeoxyribonucleotides **1** and **2** (Figure 2) were synthesized by standard automated solid-support chemistry using an Applied Biosystems Model 380B DNA synthesizer and *O*-cyanoethyl-*N*,*N*-diisopropyl phosphoramidites. The conjugate thymidine–EDTA (T*) phosphoramidite was prepared as described (Dreyer & Dervan, 1985) and incorporated at the 5′ end of oligodeoxyribonucleotides **1** and **2** with the EDTA carboxylates protected as their ethyl esters. Deprotection was carried out in 0.1 N NaOH solution at 55 °C for 24 h. Crude oligodeoxyribonucleotide products containing the 5′-terminal dimethoxytrityl protecting group were purified by reverse-phase FPLC using a ProRPC 10/10 (C_2–C_8) column (Pharmacia LKB) and a gradient of 0–40% CH_3CN in 0.1 M triethylammonium acetate, pH 7.0, detritylated using 80% aqueous acetic acid, and chromatographed a second time. Purified oligodeoxyribonucleotides were desalted on Pharmacia NAP-5 Sephadex columns and lyophilized from water twice. The concentrations of single-stranded oligodeoxyribonucleotides were determined by UV absorbance at 260 nm using extinction coefficients of 1.1×10^5 $M^{-1}\cdot cm^{-1}$ and 9.8×10^4 $M^{-1}\cdot cm^{-1}$ for **1** and **2**, respectively. Oligodeoxyribonucleotide solutions were lyophilized to dryness for storage at −20 °C.

The 5′-^{32}P-labeled duplex DNA was prepared and purified as previously described (Singleton & Dervan, 1992). The labeled DNA was resuspended in 0.5× TE buffer at a final activity of 40 000 cpm/μL for storage at 4 °C. A typical yield was 2 μg of the desired fragment with a total Cerenkov radioactivity of 6×10^6 cpm.

Quantitative Affinity Cleavage Titrations. In a typical quantitative affinity cleaving experiment, involving 15 data lanes and one control lane, a stock solution containing labeled target DNA in association buffer was prepared by mixing 0.25 M 3-(*N*-morpholino)propanesulfonic acid (MOPS, for experiments at pH 7.0–7.6) or 2-(*N*-morpholino)ethanesulfonic acid (MES, for experiments at pH 5.8–6.6) buffer at the desired pH, 0.5 M NaCl, calf thymus DNA at a concentration of 2.0 mM in base pairs, 5 mM spermine·4HCl at pH 7.0, approximately 300 000 cpm 5′-end-labeled target DNA, and enough H_2O to bring the total volume of 653 μL. The stock solution was allowed to equilibrate at room temperature for 15 min and was then distributed among 16 0.6-mL tubes in 40-μL aliquots. A dried pellet of the oligodeoxyribonucleotide-EDTA was dissolved in a solution of aqueous $Fe(NH_4)_2(SO_4)_2\cdot 6H_2O$ to produce a solution that was 80 μM in oligodeoxyribonucleotide and 88 μM in Fe(II). The oligodeoxyribonucleotide–EDTA·Fe(II) solution was allowed to equilibrate for 15 min at room temperature and was then diluted serially. To each reaction tube was added 5 μL of oligodeoxyribonucleotide–EDTA·Fe(II) at the appropriate concentration. The oligodeoxyribonucleotide–EDTA·Fe and the DNA were allowed to equilibrate for 24 h at 22 °C. The cleavage reactions were initiated by the addition of 5 μL of a 10 mM aqueous DTT solution to each tube. The reactions were incubated for 8 h at 24 °C. Final reaction conditions in 100 μL of association buffer were 50 mM MOPS (or MES) buffer at the desired pH, 100 mM NaCl, 1 mM spermine, 0.1 mM base pairs calf thymus DNA, 1 mM DTT, and approximately 17 500 cpm labeled duplex (the specific activity of the DNA varied slightly from experiment to experiment but was the same for each reaction within a given experiment and always resulted in a final target site concentration of less than 0.1 nM). The cleavage was quenched by the addition of glycogen, NaOAc (pH 5.2), and $MgCl_2$ to final concentrations of 70 μg/mL, 280 mM, and 10 mM, respectively. The DNA was precipitated with 2.5 vol of ethanol and isolated by centrifugation. The precipitate was washed once with 70% aqueous ethanol and was immediately dissolved in 20 μL of H_2O. The solutions were frozen, and the water was removed by lyophilization. The DNA in each tube was resuspended in 5 μL of formamide–TBE loading buffer and transferred to a new tube. The DNA solutions were assayed for Cerenkov radioactivity by scintillation counting and diluted to 2500 cpm/μL with more formamide–TBE loading buffer. The DNA was denatured at 90 °C for 10 min, and 5 μL of each sample was loaded onto an 8% denaturing polyacrylamide gel. The DNA cleavage products were electrophoresed in 1× TBE buffer at 60 $V\cdot cm^{-1}$. The gel was dried on a slab dryer and then exposed to a storage phosphor screen at 24 °C.

Quantitation by Storage Phosphor Technology Autoradiography. Photostimulable storage phosphor imaging plates (Kodak Storage Phosphor Screen S0230 obtained from Molecular Dynamics) were pressed flat against dried gel samples and exposed in the dark at 22 °C for 12–24 h. A Molecular Dynamics 400S PhosphorImager was used to obtain all data from the storage screens. The data were analyzed by performing volume integrations of the target site and reference blocks using the ImageQuant v. 3.0 software running on an AST Premium 386/33 computer.

Affinity Cleavage Titration Fitting Procedure. The site-specific cleavage intensities for all oligodeoxyribonucleotide–EDTA concentrations used were calculated using eq 1, where I_{tot} and I_{ref}, the cleavage intensities in the site and reference blocks, respectively, were determined from integration of storage phosphor images as described above:

$$I_{site} = I_{tot} - \lambda I_{ref} \quad (1)$$

For each experiment, λ was calculated from the average of the minimum I_{tot}/I_{ref} ratios near $\theta = 0$. For example, for the experiment whose results are shown in Figure 3, λ was calculated using the average of the ratios of I_{tot} to I_{ref} from each of the three lowest oligonucleotide concentrations and the control reaction containing no oligonucleotide (Figure 3, lanes 1–3). A theoretical binding curve was fit to the experimental data using the apparent maximum cleavage (I_{sat}) and the K_T as adjustable parameters:

$$I_{fit} = I_{sat}\frac{K_T[O]_{tot}}{1 + K_T[O]_{tot}} \quad (2)$$

The difference between I_{fit} and I_{site} for all data points was minimized using the nonlinear least-squares fitting procedure of KaleidaGraph (version 2.1; Abelbeck Software) running on a Macintosh IIfx computer. All data points were included in the fitting procedure unless visual inspection of the computer image from a storage phosphor screen revealed a flaw at either the target site or reference blocks or unless the I_{site} value for a single lane was greater than two standard errors away from

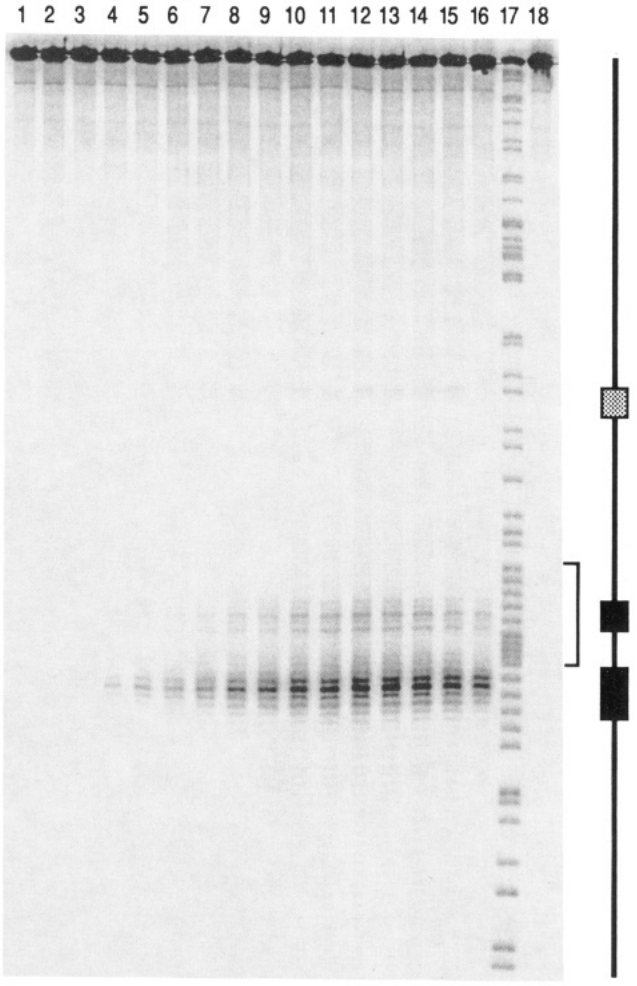

FIGURE 3: Gray-scale representation of a storage phosphor autoradiogram of an 8% denaturing polyacrylamide gel used to separate the cleavage products generated by **1** during a quantitative affinity cleavage titration experiment performed in association buffer (100 mM Na^+, 1 mM spermine, 50 mM MOPS) at 22 °C and pH 7.6. There are 224 levels of gray representing a 50-fold change in the signal from the lowest (120 arbitrary units, white) to highest (6000 arbitrary units, black) intensities. The bracket on the right side of the autoradiogram encloses the nucleotide positions of the 15 bp duplex target site. The bar drawn on the right of the autoradiogram indicates the bands used to measure I_{tot} (black boxes) and the bands used to measure I_{ref} (gray box). (Lanes 1–16) DNA affinity cleavage products produced by **1** at various concentrations: no oligonucleotide (lane 1); 10 nM (lane 2); 20 nM (lane 3); 40 nM (lane 4); 80 nM (lane 5); 100 nM (lane 6); 200 nM (lane 7); 400 nM (lane 8); 800 nM (lane 9); 1.0 μM (lane 10); 2.0 μM (lane 11); 4.0 μM (lane 12); 8.0 μM (lane 13); 10 μM (lane 14); 20 μM (lane 15); 40 μM (lane 16). (Lane 17) Products of an adenine-specific sequencing reaction. (Lane 18) Intact 5′-labeled duplex.

both values from the neighboring lanes. Data from experiments for which fewer than 80% of the data lanes were usable were discarded. The goodness of fit of the binding curve to the data points was judged by the χ^2 criterion (Shoemaker et al., 1981), and fits were judged acceptable for $\chi^2 \leq 1.0$. Correlation coefficients reported for acceptable fits were ≥ 0.95.

All fits described in this text were performed without weighting the data points. When the formula for propagation of errors is used (Shoemaker et al., 1981), the following equation describing the uncertainty in I_{site} can be derived:

$$\epsilon(I_{site}) = \rho[I_{tot}^2 + 3(\lambda I_{ref})^2]^{1/2} \quad (3)$$

where ρ describes the experimental reproducibility for manipulating the labeled DNA and integrating the cleavage intensities. The value $\rho = 0.1$ was obtained from the ratio of the standard deviation to the mean for measured I_{site} values at a single oligonucleotide–EDTA·Fe concentration. A fit of data points using statistical weighting and the described uncertainties results in uncertainties in the fitting parameter K_T that were typically 20–30% of the value of K_T.

Repeat experiments using a particular oligodeoxyribonucleotide–EDTA·Fe were performed using different serial dilutions of the oligonucleotide and different preparations of 5′-end-labeled duplex DNA. Standard deviations among different experimental measurements of K_T were typically 30–50% of the mean K_T. All K_T values reported in the text or tables are means of three to five experimental observations ± SEM.

RESULTS

Oligonucleotide–EDTA Equilibrium Association Constants. Previous experiments demonstrated that the equilibrium association constant for the binding of an oligonucleotide–EDTA·Fe to an individual DNA site can be measured using quantitative affinity cleavage titration (Singleton & Dervan, 1992). Because a description and analysis of this method has been presented, only a summary of the rationale and design of the experimental protocol is presented below.

The equilibrium complexation of an oligonucleotide–EDTA·Fe (O) with duplex DNA (D) containing a double-helical target site to form a local triple-helical structure (T), followed by affinity cleavage of the bound target into shorter product fragments (P_{cl}), is described by

$$O + D \overset{K_T}{\rightleftharpoons} T \overset{k_{cl}}{\rightarrow} P_{cl} \quad (4)$$

where K_T represents the equilibrium association constant and k_{cl} the pseudo-first-order rate constant for the formation of the cleavage products from the complex, T. K_T can be expressed as a function of θ, the fraction of duplex target sites occupied by O, and the equilibrium concentration of free (unbound) O, $[O]_{eq}$:

$$K_T = \frac{\theta}{1-\theta}\frac{1}{[O]_{eq}} \quad (5)$$

We have shown that the apparent fraction bound, θ_{app}, can be related to the intensity of bands proximal to the oligonucleotide-binding site (I_{site}) on a phosphor storage image of a polyacrylamide gel used to separate cleavage products from intact duplex. Accordingly, for a series of affinity cleavage experiments in which the solution conditions, concentration of duplex, reaction volume, and reaction time are constant,

$$\theta_{app} = I_{site}I_{sat}^{-1} \quad (6)$$

where I_{sat} is the intensity of cleavage produced when $\theta \approx 1$. Because radiolabeled duplex DNA of high specific activity is used in the experiments, the concentration of duplex can be lowered such that $[D]_{tot}$ is less than 5% of the lowest $[O]_{tot}$ to be used. With these concentrations, we can equate $[O]_{tot}$ to $[O]_{eq}$ because, even at $\theta \approx 1$, the amount of bound O will be negligible. Substitution of $I_{site}I_{sat}^{-1}$ for θ and $[O]_{tot}$ for $[O]_{eq}$ in eq 5, followed by rearrangement, yields an expression for I_{site}:

$$I_{site} = I_{sat}\frac{K_T[O]_{tot}}{1 + K_T[O]_{tot}} \quad (7)$$

Hence, by measuring the site-specific affinity cleavage

produced by bound oligonucleotide–EDTA·Fe as a function of $[O]_{tot}$, empirical titration binding isotherms can be constructed to determine K_T from nonlinear least-squares analysis of the $([O]_{tot},I_{site})$ data points. From previous work, we have shown that quantitative affinity cleavage titration affords equilibrium association constants that are identical, within experimental uncertainty, to those obtained from the established DNase I footprint titration method of Brenowitz et al. (1986) (Singleton & Dervan, 1992). Moreover, covalent attachment of EDTA·Fe to thymine at the 5′-terminus of an oligodeoxyribonucleotide does not have a measurable effect on the binding constant (Singleton & Dervan, 1992).

Association Constants as a Function of pH. To assess the influence of pH on the energetics of oligonucleotide-directed triple hexix formation, the equilibrium association constants for oligonucleotide–EDTA conjugates binding to a 339 bp DNA duplex containing a 15 bp target sequence (Figure 2) were measured in buffers of different pH. At a given pH, ^{32}P 5′-end-labeled DNA (<5 pM) and various concentrations of oligonucleotide–EDTA·Fe (100 pM–10 μM) were mixed in association buffer (100 mM Na^+, 1 mM spermine, and 50 mM MES or MOPS) at 22 °C. Only after the association reactions has been allowed to reach equilibrium over 24 h was DTT (1 mM final concentration) added to initiate the EDTA·Fe-mediated DNA cleavage. The reactions were allowed to proceed for 8 h at 22 °C, allowing a maximum site-specific cleavage yield of about 15%. The products were separated by PAGE under strand-denaturing conditions. A storage phosphor autoradiogram from a typical experiment using of oligonucleotide–EDTA·Fe **1** (Figure 2) at pH 7.6 is shown in Figure 3.

The amounts of radiolabeled DNA in the bands at the target cleavage site (Figures 2 and 3) and at a reference site (Figure 3) were measured from storage phosphor autoradiograms, and I_{site} for each $[O]_{tot}$ was calculated using eq 1. The $([O]_{tot},I_{site})$ data points were fitted using a nonlinear least-squares method and eq 2, with K_T and I_{sat} as adjustable parameters. The data points obtained for **1** at pH 7.6, 6.6, 6.2, and 5.8 were averaged from several experiments and are plotted along with average best-fit titration binding isotherms in Figure 4, panels A and C–E. The average data points and best fit curve for **1** at pH 7.0 were published previously (Singleton & Dervan, 1992) and have been reproduced in Figure 4B. The corresponding averaged data and best-fit isotherms for **2** are presented in Figures 4F–J. The mean K_T values obtained from the analyses of these data are contained in Table I. The isotherms (Figure 4) and the K_T values (Table I) measured at different pH's demonstrate that the association of both **1** and **2** are driven toward triple helix formation at lower pH. The trend of increasing triple helix stability with increasingly acidic pH, which is consistent with the presumed requirement for cytosine N3 protonation, is more clearly indicated by the plots of K_T versus pH displayed in Figure 5.

An expression for the pH dependence of triple helix formation follows from a general theoretical description of a pH-dependent equilibrium (Edsall & Gutfreund, 1983; Lyamichev et al., 1988). The association constant may be factored into two terms, one of which arises from the stability constant for the unprotonated triple-helical complex and the other from stabilization of the complex resulting from equilibrium protonation of the complex:

$$K_T = K_T^{\circ}(1 + 10^{pK_{aT}-pH})^p \quad (8)$$

where K_T° is the association constant for the unprotonated oligonucleotide, p is the number of potential protonation sites

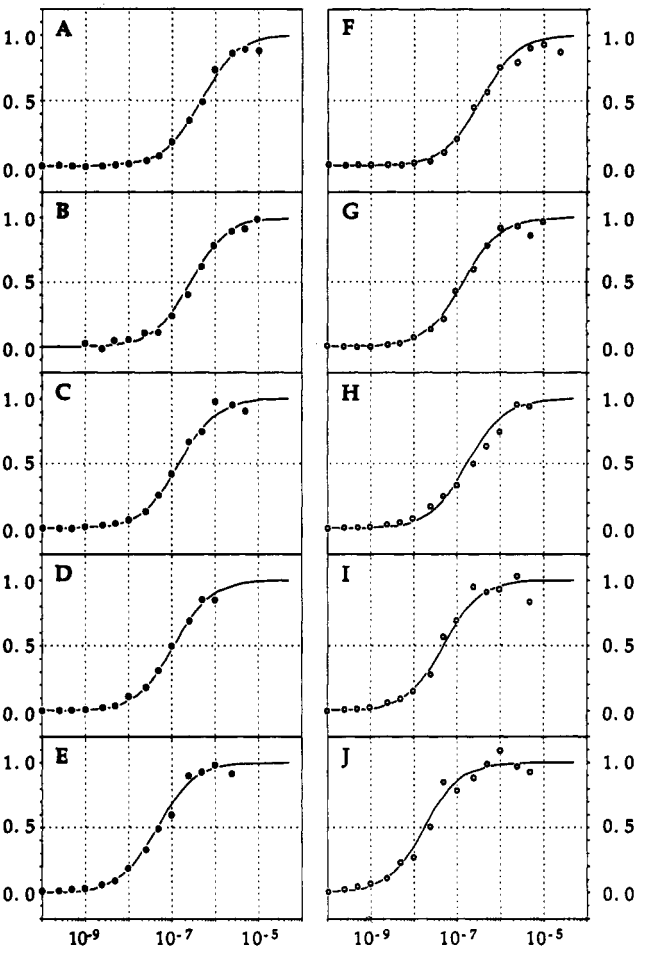

FIGURE 4: Data for quantitative affinity cleavage experiments involving oligodeoxyribonucleotides **1** (●) or **2** (○) in association buffer (22 °C) at pH 7.6 (A, F), 7.0 (B, G), 6.6 (C, H), 6.2 (D, I), and 5.8 (E, J). The data points represent the average site-specific cleavage signal intensities from three to five experiments. The sigmoidal curves show the titration binding isotherms plotted using the mean values of K_T for **1** and **2** (Table I) and eq 2. The data points were normalized using I_{sat} from each experiment, and the binding curves were subsequently normalized using I_{sat} = 1 for eq 2.

Table I: Influence on pH on K_T and ΔG_T at 22 °C[a]

	1 (C, T)		**2** (m^5C, T)	
pH	K_T (M^{-1})	ΔG_T (kcal·mol^{-1})	K_T (M^{-1})	ΔG_T (kcal·mol^{-1})
7.6	2.2 (±0.4) × 10^6	−8.5 (±0.2)	2.8 (±1.0) × 10^6	−8.7 (±0.4)
7.0	3.7 (±1.1) × 10^6 [b]	−8.9 (±0.3)[b]	7.1 (±2.8) × 10^6	−9.2 (±0.4)
6.6	7.0 (±0.9) × 10^6	−9.2 (±0.1)	5.6 (±1.3) × 10^6	−9.1 (±0.2)
6.2	8.8 (±2.6) × 10^6	−9.4 (±0.3)	2.0 (±0.4) × 10^7	−9.8 (±0.2)
5.8	2.2 (±0.5) × 10^7	−9.9 (±0.2)	5.5 (±1.7) × 10^7	−10 (±0.3)

[a] Values reported in the table are mean values measured from quantitative affinity cleavage experiments performed in association buffer (100 mM Na^+, 1 mM spermine, and 50 mM MOPS or MES buffer) at the indicated pH. [b] These values were taken from previously published experiments performed under the same conditions (Singleton & Dervan, 1992).

(i.e., the number of cytosine residues in the oligonucleotide), and K_{aT} is the mean acid dissociation constant of those sites (i.e., C+GC triplets). The (pH, K_T) data points in Figure 5 were fitted to eq 8 with p = 5 and K_T° and pK_{aT} as adjustable parameters. The best-fit curves to the data for both **1** and **2** are plotted in Figure 5. The parameters given by the fitting, summarized in Table II, yield an estimated value of 5.5 for the pK_{aT} of the triple helix formed upon binding of **1** to its double-helical target and a value of 5.7 for the pK_{aT} of the triple helix with **2** bound. Interestingly, a pK_{aT} in this range

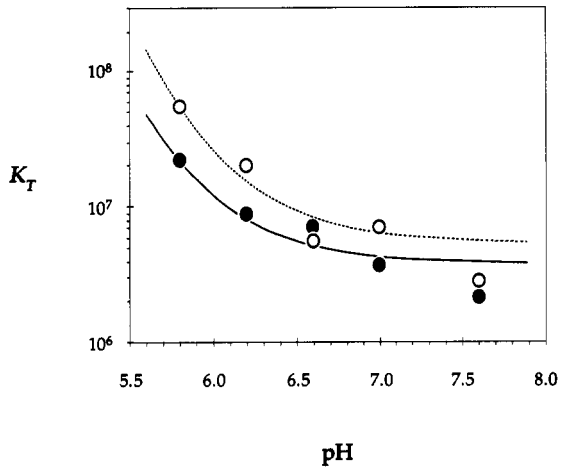

FIGURE 5: Plots of the mean values (logarithmic scale) of K_T for 1 (●) and 2 (○) as a function of pH and the nonlinear least-squares fitted curves (solid and dotted lines, respectively) generated using eq 8 with $K_T°$ and pK_{aT} as adjustable parameters. The parameters obtained from the fitting procedure are reported in Table II.

Table II: Parameters Describing the pH Dependence of K_T at 22 °C[a]

oligonucleotide	site of protonation[b]	$K_T°$ (M^{-1})	pK_{aT}	$K_{aO}K_{aT}^{-1}$ [c]	$-RT \ln (K_{aO}K_{aT}^{-1})$ (kcal·mol^{-1})
1	C·GC	3.8×10^6	5.5	13	−1.5
2	m^{5}C·GC	5.4×10^6	5.7	20	−1.8

[a] The parameters were obtained by fitting the (K_T, pH) data points shown in Figure 5 to eq 8. [b] The site of protonation formed upon binding of the oligonucleotide listed in the first column to the double-helical target site. [c] The ratio of acid dissociation constants is obtained using $pK_{aO} = 4.4$ as described in the text (eq 11).

suggests that the triple helix is not fully protonated near pH 7. A model of the triple helix in which the degree of protonation changes with pH is consistent with the large decrease in the lifetime of a triple-helical complex observed when the solution pH was raised from 6.8 to 7.2 (Maher et al., 1990).

DISCUSSION

The Influence of pH on the Association Constant. The energetics of site-specific oligonucleotide-directed triple helix formation have been analyzed by quantitative affinity cleavage titration as a function of pH. Over the pH range of 5.8–7.6, K_T for **1** decreases by a factor of 10, while K_T for **2** decreases 20-fold over the same range. Least-squares fitting analysis of the K_T versus pH data afforded estimates of $pK_{aT} = 5.5$ and $K_T° = 3.8 \times 10^6$ M^{-1} for the triple helix formed by association of **1** to the double-helical target site. The pK_{aT} value is near the semiprotonation points for oligonucleotide triplexes measured to be 5.6, 5.8, and 6.2 by ethidium bromide fluorescence (Callahan et al., 1991), UV absorption spectroscopy (Xodo et al., 1991), and CD spectroscopy (Callahan et al., 1991), respectively. A similar analysis revealed that $pK_{aT} = 5.7$ and $K_T° = 5.4 \times 10^6$ M^{-1} for the triple-helical structure formed upon binding of **2**. This value is considerably lower than the value of 6.8 measured using a UV spectroscopic technique for an oligonucleotide triplex (Xodo et al., 1991). The physical model characterized by eq 8 describes the effect of pH on a global equilibrium process rather than an intrinsic pK_a at a single atom as could be measured using NMR spectroscopy. The fact that other pH-dependent processes, including spermine binding and conformational changes in both the duplex and triplex, may be occurring under the conditions described herein adds complexity to the analysis. The polyelectrolyte behavior of the 339 bp double-helical DNA molecule containing the target site may result in a buffering of the pH of the local solution environment near the duplex (Slonitskii & Kuptsov, 1988). Such behavior would likely result in a decreased dependence of the triplex stability on bulk pH near pH 7 and an increased value for the apparent $K_T°$. Despite the complexity inherent in this analysis, the apparent pK_{aT} values measured using quantitative affinity cleavage titration allow an accurate characterization of the pH dependence of oligonucleotide-directed triple helix formation on large DNA.

A quantitative estimate of the stabilization of the triple helix resulting from protonation was derived from the pH-dependence data and the following thermodynamic cycle:

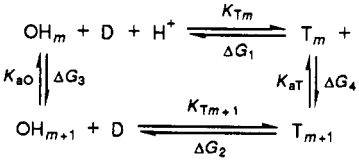

(9)

where OH_m and OH_{m+1} represent oligonucleotides with m and $m+1$ protonated cytosines, respectively, T_m and T_{m+1} represent triplexes with m and $m+1$ protonated C+GC base triads, respectively, K_{aO} and K_{aT} are the acid dissociation constants for the oligonucleotide and triplex, respectively, and K_{Tm} and K_{Tm+1} are the association constants for triple helix formation involving oligonucleotides with m and $m+1$ protonated cytosines, respectively ($0 \leq m \leq p$). Because the equilibria in eq 9 represent a cycle, the following relationships between the free energies and the equilibrium constants may be written:

$$\Delta G_4 - \Delta G_3 = \Delta G_2 - \Delta G_1 \tag{10}$$

$$\frac{K_{aO}}{K_{aT}} = \frac{K_{Tm+1}}{K_{Tm}} \tag{11}$$

Equations 10 and 11 equate the change in the pK_a of cytosine N3 upon binding of the oligonucleotide to its double-helical target site with the stabilization of the triple helix resulting from the addition of one proton to an acceptor site in the triplex to form a C+GC base triplet. Xodo et al. (1991) have determined the pK_a's for both of two single-stranded pyrimidine oligonucleotides containing C or m^{5}C residues to be 4.4 ± 0.2. Because the pK_as of cytosine residues in a single-stranded oligonucleotide are not expected to be strongly perturbed by the adjacent nucleotides, the ratios of equilibrium constants (eq 11) for **1** and **2** were estimated using $pK_{aO} = 4.4$ and included in Table II.

The K_{Tm+1}/K_{Tm} ratios suggest that the protonated state of cytosine is stabilized by 1.5 kcal·mol^{-1} when the proton is placed in the acceptor site between cytosine N3 and guanine N7 in the triple helix (Figure 1), while N3-protonated 5-methylcytosine is stabilized by 1.8 kcal·mol^{-1} in the triplex. At least two sources give rise to this stabilization. Clearly, interactions such as hydrogen bonding between the cytosine heterocycle and proximal bases will stabilize the protonated state of cytosine. Charge–charge interactions may also play a key role in this phenomenon. Investigations by Callahan et al. (1991) on the pH-dependent formation of oligonucleotide triplexes suggest that the stabilization energy resulting from Coulombic attraction between the positively charged N3 of a protonated cytosine and an anionic phosphate group of the duplex may be up to 0.5 kcal·mol^{-1}. The dependence of the

stability of the triple helix on the solution pH is remarkable. The addition of one proton to a C·GC acceptor site in a local triple-helical structure stabilizes the structure by 1.5 kcal·mol^{-1}, while the addition of one C+GC and one T·AT triplet to the structure at pH 7.0 confers a stabilization of only 0.5 kcal·mol^{-1} (Singleton & Dervan, 1992).

The Influence of Substitution at C5 of Cytosine. An analysis of the stabilization conferred by C → m^{5}C substitution on oligonucleotide-directed triple helix formation is achieved by comparing the K_T values for **1** and **2**. The plot of K_T versus pH (Figure 5) demonstrates that, for the binding of **1** over the range of pH 5.8–7.6, the use of oligonucleotide **2** extends the pH range for forming a triple helix of equivalent stability by 0.5–1.0 units. This finding is consistent with earlier studies comparing relative cleavage efficiencies produced at single concentrations of oligonucleotide–EDTA·Fe (Povsic & Dervan, 1989). The methyl substitutent at C5 of cytosine increases the apparent pK_{aT} by 0.2 units and increases $K_T°$ by a factor of 1.5. Although the uncertainty in the fitted pK_{aT} values is likely similar in magnitude to the difference between them (ΔpK_{aT} = 0.2), the increase in the pK_{aT} afforded by the C → m^{5}C substitution is modest compared to that observed (ΔpK_{aT} = 1.0) for the triplexes formed upon binding of 5′-CTTC-CTCCTCT-3′ or 5′-m^{5}CTTm^{5}Cm^{5}CTm^{5}Cm^{5}CTm^{5}CT-3′ to an oligonucleotide duplex target (Xodo et al., 1991). Among the possible explanations for the apparent difference in ΔpK_{aT} are (i) the methods used to measure pK_{aT}; (ii) the sequence dependence of pK_{aT}; and (iii) a combination of both. Recently, Hampel et al. (1991) demonstrated that the method used to measure the apparent pK_{aT} of the polymeric triplex $[d(TC)]_n$·$[d(GA)]_n$·$[d(CT)]_n$ strongly affected the measured value. In fact, the pK_{aT} determined by adding base to the triplex formed at acidic pH was ~1.5 units higher than that measured under equilibrium conditions. Presumably, once formed at acidic pH, the triplex remains as a "metastable" complex for a length of time dependent on the dissociation rate of the complex. While it has been shown that 5-methylcytosine is required for a 21-mer oligonucleotide to protect an overlapping restriction endonuclease site from cleavage by the enzyme in a kinetic assay (Maher et al., 1990), data are not yet available to compare the dissociation rates of triplexes containing cytosines or 5-methylcytosines in the third strand. An alternative explanation for the observed differences in ΔpK_{aT} is the possibility of a sequence-dependent pK_{aT}. The earlier work (Xodo et al., 1991) involved triple-helical complexes wherein four of the six X^{5}C+GC triplets were flanked on one side by X^{5}C+GC triplets and a fifth one is at the 5′-terminus, while the complexes described here contain only internal X^{5}C+GC triplets flanked by T·AT triplets. Because the stabilities of triplexes containing C+GC triplets have been shown to be dependent on the base triplets flanking the C+GC triplets (Kiessling et al., 1992), we anticipate that the pK_{aT} values for these complexes may be sequence-dependent and that the effect of the functional group at C5 of the cytosine heterocycle may also be influenced by the nearest neighbor triplets.

A comparison of the ΔG_T values for formation of the triple-helical structures involving **1** and **2** (Table I) reveals that substitution of a methyl group at C5 of cytosine stabilizes the triple-helical complex by 0.1–0.4 kcal·mol^{-1} over the pH range of 5.8–7.6. Replacement of the hydrogen atom normally attached to C5 of cytosine with an electron-donating methyl substituent is expected to slightly increase the pK_a of the base in both the free and complexed oligonucleotides, making protonation of the m^{5}C residue easier while reducing its hydrogen-bond donating ability from the protonated N3; however, the differences in the pK_a's of cytosine and 5-methylcytosine in nucleosides and oligonucleotides are measured to be ≤0.1 units (Sober, 1970; Xodo et al., 1991). On the basis of differential scanning calorimetric measurements which demonstrated that a C → m^{5}C substitution in the third strand results in a decreased denaturation enthalpy, Xodo et al. (1991) reasoned that methylation induces a release of water molecules from the helix, thereby contributing a positive entropy change. While differences in solvation in the complexes formed upon binding of **1** and **2** may play a role in the differential stabilities of the two triple-helical structures, it is interesting that the free 5-methylcytosine base is more soluble in water than cytosine (Sowers et al., 1987b).

In addition to change in hydrogen bonding and solvation, another likely source of the stabilizing influence of a C5-methyl group may arise from increased base-stacking interactions. The importance of base stacking in nucleic acid helical complexes was demonstrated by early investigations concerning the role of organic solvents in denaturing double-helical DNA (Hanlon, 1966). These studies implicated dispersion forces, a key component of stacking, as a stabilizing factor in the double helix. Stacking energies, which arise from dispersion and induced dipole interactions (DeVoe & Tinoco, 1962; Ornstein et al., 1978), have been shown to correlate reasonably well with the polarizabilities of the interacting heterocycles (Broom et al., 1967; Ts'o, 1968; Nakano & Igarichi, 1970; Lawaczek & Wagner, 1974; Sowers et al., 1987b; Darzynkiewicz & Lönnberg, 1989). Moreover, methylation of the stacked bases increases the interaction energies (Broom et al., 1967; T'so, 1968; Nakano & Igarichi, 1970; Sowers et al., 1987b). In fact, substitution of a methyl group at C5 of cytosine increases its molecular polarizability (Miller & Savchik, 1979; Sowers et al., 1987b) and increases the free energy of stacking of cytosine with adenine in water by 0.2 kcal·mol^{-1} (Sowers et al., 1987b). Models of stacked base triplets constructed using A′-form (Figure 6A) or B-form (Figure 6B) helical turn angles suggest that the C5-substitutent is positioned to play a role in stacking with an adjacent pyrimidine in the third strand of a triple helix. The observation that local triple-helical structures containing m^{5}C in the third strand are stabilized relative to those containing C in the third strand by a similar amount over a range of pH, including those where the triplexes may not be fully protonated, is consistent with the interpretation that the methyl group may stabilize the complex without *directly* influencing the protonation event (e.g., through increased stacking energy).

In addition to an equilibrium thermodynamic stabilization, the C5-methyl substitution may have a dynamic effect on the triple-helical structure. It has been recognized that protonation of pyrimidines diminishes pyrimidine–pyrimidine stacking interactions in the crystalline state (Bugg et al., 1971; Saenger, 1984; Padmaja et al., 1991). This proton-induced destacking may account for the observation that third-strand cytosine N3 protons exchange more rapidly with solvent and that their NMR signals disappear more rapidly with increased temperature than thymine N3 protons (Rajagopal & Feigon, 1989b). Furthermore, an unprotonated C·GC base triplet may have a shorter intrinsic lifetime than a T·AT base triplet, since the former has only a single hydrogen bond. Increased stacking through the interaction of the C5-methyl group with the polarizable π-system of the neighboring heterocycle (Figure 6) may hold an unprotonated m^{5}C base in better position for maintaining its lone hydrogen bond and may reduce any tendency for a protonated m^{5}C heterocycle to unstack. A similar dynamic phenomenon has been observed in a com-

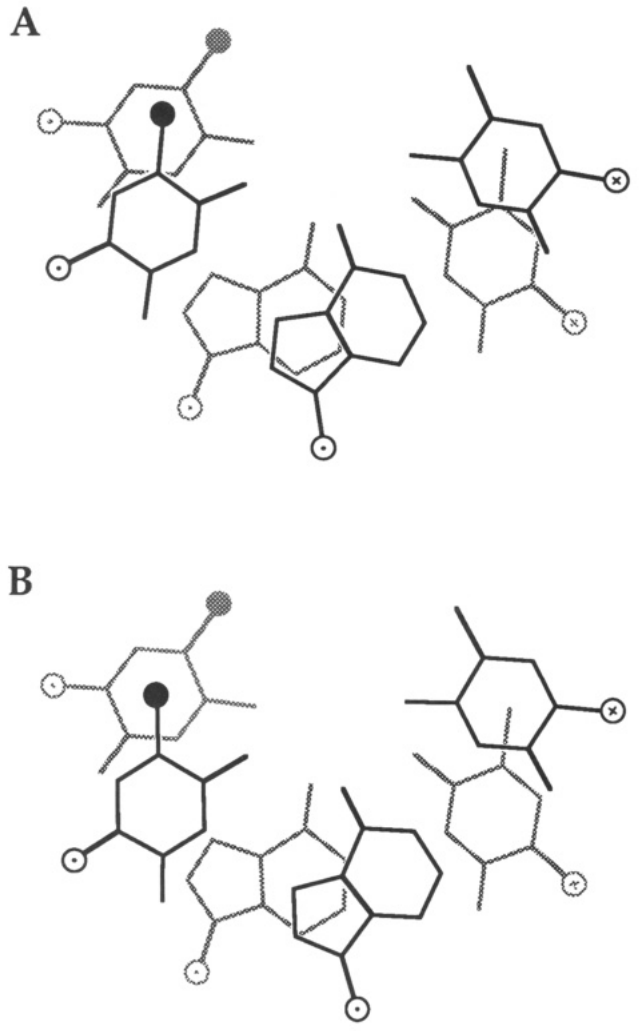

FIGURE 6: (A) Base-stacking configurations drawn using the idealized helical parameters generated from diffraction data for fibers of the polymeric triplex $(T{\cdot}AT)_n$ (Arnott et al., 1976). The C1′ atoms of the deoxyribose sugars are represented by the open circles. The 5′ → 3′ polarity of the strands is indicated by the symbols ⊗ (into the plane of the page) and ⊙ (out of the plane of the page). The filled circles indicate the positions of the methyl groups at C5 of thymines in the third strand. (B) Base-stacking model generated as above except that the helical turn angle per residue for B-form nucleic acids was used (Saenger, 1984).

parison of the NMR behavior of double-helical DNAs containing thymine or 5-fluorouracil bases (Sowers et al., 1987a). A complete elucidation of the equilibrium and dynamic influences of the C → m^5C substitution on a triple-helical structure must await more direct physical characterization.

CONCLUSIONS

Quantitative affinity cleavage titration has been used to measure the equilibrium constants for the formation of a local triple-helical complex a single site within large DNA over the pH range of 5.8–7.6 at 22 °C (100 mM Na^+ and 1 mM spermine). The triple helix formed upon binding of **1** to the double-helical target site is stabilized by 1.4 kcal·mol^{-1} as the pH is lowered from 7.6 to 5.8. Replacement of the five cytosine residues in the third strand with 5-methylcytosine residues stabilizes the triple-helical DNA complex by 0.1–0.4 kcal·mol^{-1} over this pH range, resulting in a modest increase in the pK_{aT} of the triple helix from 5.5 to 5.7. The importance of third-strand protonation and the potential contributions of base stacking forces to the energetics of pyrimidine oligonucleotide-directed triple helix formation offer intriguing possibilities for the direction of synthetic efforts toward novel nucleosides as well as for experiments to elucidate further the structure and stability of triple-helical complexes.

REFERENCES

Arnott, S., Bond, P. J., Selsing, E., & Smith, P. J. C. (1976) *Nucleic Acids Res. 3*, 2459–2470.

Beal, P. A., & Dervan, P. B. (1991) *Science 251*, 1360–1363.

Brenowitz, M., Senear, D. F., Shea, M. A., & Ackers, G. K. (1986) *Methods Enzymol. 130*, 132–181.

Broom, A. D., Schweizer, M. P., & Ts'o, P. O. P. (1967) *J. Am. Chem. Soc. 89*, 3612–3622.

Bugg, C. E., Thomas, J. M., Sundaralingam, M., & Rao, S. T. (1971) *Biopolymers 10*, 175–219.

Callahan, D. E., Trapane, T. L., Miller, P. S., Ts'o, P. O. P., & Kan, L.-S. (1991) *Biochemistry 30*, 1650–1655.

Collier, D. A., Thuong, N. T., & Helene, C. (1991) *J. Am. Chem. Soc. 113*, 1457–1458.

Cooney, M., Czernuszewicz, G., Postel, E. H., Flint, S. J., & Hogan, M. E. (1988) *Science 241*, 456–459.

Darzynkiewicz, E., & Lönnberg, H. (1989) *Biophys. Chem. 33*, 289–293.

de los Santos, C., Rosen, M., & Patel, D. (1989) *Biochemistry 28*, 7282–7289.

DeVoe, H., & Tinoco, I. (1962) *J. Mol. Biol.* , 500–517.

Dreyer, J. B., & Dervan, P. B. (1985) *Proc. Natl. Acad. Sci. U.S.A. 82*, 968.

Duval-Valentin, G., Thuong, N. T., & Helene, C. (1992) *Proc. Natl. Acad. Sci. U.S.A. 89*, 504–508.

Edsall, J. T., & Gutfreund, H. (1983) *Biothermodynamics: The Study of Biochemistry Processes at Equilibrium*, John Wiley & Sons, New York.

Felsenfeld, G., Davies, D. R., & Rich, A. (1957) *J. Am. Chem. Soc. 79*, 2023–2024.

Gait, M. J. (1984) *Oligonucleotide Synthesis: A Practical Approach*, IRL Press, Oxford.

Grigoriev, M., Praseuth, D., Robin, P., Hemar, A., Saison-Behmoaras, T., Dautry-Varsat, A., Thuong, N. T., Helene, C., & Harel-Bellan, A. (1992) *J. Biol. Chem. 267*, 3389–3395.

Hampel, K. J., Crosson, P., & Lee, J. S. (1991) *Biochemistry 30*, 4455–4459.

Hanlon, S. (1966) *Biochem. Biophys. Res. Commun. 23*, 861–867.

Howard, F. B., Frazier, J., Lipsett, M. N., & Miles, H. T. (1964) *Biochem. Biophys. Res. Commun. 17*, 93–102.

Kiessling, L. L., Griffin, L. C., & Dervan, P. B. (1992) *Biochemistry 31*, 2829–2834.

Koh, J. S., & Dervan, P. B. (1992) *J. Am. Chem. Soc. 114*, 1470–1478.

Krawczyk, S. H., Milligan, J. F., Wadwani, S., Moulds, C., Froehler, B. C., & Matteucci, M. D. (1992) *Proc. Natl. Acad. Sci. U.S.A. 89*, 3761–3764.

Lawaczeck, R., & Wagner, K. G. (1974) *Biopolymers 13*, 2003–2014.

LeDoan, T., Perrouault, L., Praseuth, D., Habhoub, N., Decout, J.-L., Thuong, N. T., Lhomme, J., & Helene, C. (1987) *Nucleic Acids Res. 15*, 7749–7760.

Lee, J. S., Johnson, D. A., & Morgan, A. R. (1979) *Nucleic Acids Res. 6*, 3073–3091.

Lee, J. S., Woodsworth, M. L., Latimer, L. J. P., & Morgan, A. R. (1984) *Nucleic Acids Res. 12*, 6603–6614.

Live, D. H., Radhakrishnan, I., Misra, V., & Patel, D. J. (1991) *J. Am. Chem. Soc. 113*, 4687–4688.

Lyamichev, V. I., Mirkin, S. M., Frank-Kamenetskii, M. D., & Cantor, C. R. (1988) *Nucleic Acids Res. 16*, 2165–2178.

Maher, L. J., III, Wold, B., & Dervan, P. B. (1989) *Science 245*, 725–730.

Maher, L. J., III, Dervan, P. B., & Wold, B. (1990) *Biochemistry 29*, 8820–8826.

Mergny, J.-L., Sun, J.-S., Rougee, M., Montenay-Garestier, T., Barcelo, F., Chomilier, J., & Helene, C. (1991) *Biochemistry 30*, 9791–9798.
Miller, K. J., & Savchik, J. A. (1979) *J. Am. Chem. Soc. 101*, 7206–7213.
Moser, H. E., & Dervan, P. B. (1987) *Science 238*, 645–650.
Nakano, N. I., & Igarashi, S. J. (1970) *Biochemistry 9*, 577–583.
Ono, A., Ts'o, P. O. P., Lou-sing, K. (1991) *J. Am. Chem. Soc. 113*, 4032–4033.
Ornstein, R. L., Rein, R., Breen, D. L., & MacElroy, R. D. (1978) *Biopolymers 17*, 2341–2360.
Padmaja, N., Ramakujmar, S., & Viswamitra, M. A. (1991) *Acta Crystallogr. 47*, 1445–1448.
Plum, G. E., Park, Y.-W., Singleton, S. F., Dervan, P. B., & Breslauer, K. J. (1990) *Proc. Natl. Acad. Sci. U.S.A. 87*, 9436–9440.
Povsic, T. J., & Dervan, P. B. (1989) *J. Am. Chem. Soc. 111*, 3059–3061.
Praseuth, D., Perrouault, L., LeDoan, T., Chassignol, M., Thuong, N., & Helene, C. (1988) *Proc. Natl. Acad. Sci. U.S.A. 85*, 1349–1353.
Rajagopal, P., & Feigon, J. (1989a) *Biochemistry 28*, 7859–7870.
Rajagopal, P., & Feigon, J. (1989b) *Nature 339*, 637–640.
Roberts, R. W., & Crothers, D. M. (1991) *Proc. Natl. Acad. Sci. U.S.A. 88*, 9397–9401.
Saenger, W. (1984) *Principles of Nucleic Acid Structure*, Springer-Verlag, New York.
Sambrook, J., Fritsch, E. F., & Maniatis, T. (1989) *Molecular Cloning*, 2nd ed., Cold Spring Harbor Laboratory, Cold Spring Harbor, NY.
Shoemaker, D. P., Garland, C.W., Steinfeld, J. I., & Nibler, J. W. (1981) *Experiments in Physical Chemistry*, McGraw-Hill, New York.
Singleton, S. F., & Devan, P. B. (1992) *J. Am. Chem. Soc. 114*, 6957–6965.
Slonitskii, S. V., & Kuptsov, V. Y. (1988) *Mol. Biol. 22*, 593–608.
Sober, H. A. (1970) *Handbook of Biochemistry. Selected Data for Molecular Biology*, CRC Press, Cleveland, OH.
Sowers, L. C., Eritja, R., Kaplan, B. E., Goodman, M. F., & Fazakerley, G. V. (1987a) *J. Biol. Chem. 262*, 15436–15442.
Sowers, L. C., Shaw, B. R., & Sedwick, W. D. (1987b) *Biochem. Biophys. Res. Commun. 148*, 790–794.
Strobel, S. A., & Dervan, P. B. (1991) *Nature 350*, 172–174.
Strobel, S. A., Doucette-Stamm, L. A., Riba, L., Housman, D. E., & Dervan, P. B. (1991) *Science 254*, 1639–1642.
Ts'o, P. O. P. (1968) in *Molecular Associations in Biology* (Pullman, B., Ed.) pp 39–75, Academic Press, New York.
Xodo, L. E., Manzini, G., Quadrifoglio, F., van der Marel, G. A., & van Boom, J. H. (1991) *Nucleic Acids Res. 19*, 5625–5631.